BBA - Molecular Cell Research 1864 (2017) 1413–1424

Contents lists available at ScienceDirect

BBA - Molecular Cell Research

journal homepage: www.elsevier.com/locate/bbamcr

Cortical cytoskeleton dynamics regulates plasma membrane calcium ATPase isoform-2 (PMCA2) activity

Marianela G. Dalghi[a,b,*], Mariela Ferreira-Gomes[a], Nicolás Montalbetti[b], Alexandre Simonin[b], Emanuel E. Strehler[c,d], Matthias A. Hediger[b], Juan Pablo Rossi[a,**]

[a] IQUIFIB – Instituto de Química y Fisicoquímica Biológicas, Conicet/UBA, Junín 956, 1113 Buenos Aires, Argentina
[b] Institute of Biochemistry and Molecular Medicine, Swiss National Centre of Competence in Research, NCCR TransCure, University of Bern, Bühlstrasse 28, 3012 Bern, Switzerland
[c] Department of Biochemistry and Molecular Biology, Mayo Clinic College of Medicine, Rochester, USA
[d] Department of Biomedicine, University of Basel, Switzerland

ARTICLE INFO

Keywords:
PMCA2
Actin
Microtubules
Cortical cytoskeleton
Modulation

ABSTRACT

We have previously shown that purified actin can directly bind to human plasma membrane Ca^{2+} ATPase 4b (hPMCA4b) and exert a dual modulation on its Ca^{2+}-ATPase activity: F-actin inhibits PMCA while short actin oligomers may contribute to PMCA activation. These studies had to be performed with purified proteins given the nature of the biophysical and biochemical approaches used. To assess whether a functional interaction between the PMCAs and the cortical cytoskeleton is of physiological relevance, we characterized this phenomenon in the context of a living cell by monitoring in real-time the changes in the cytosolic calcium levels ($[Ca^{2+}]_{CYT}$). In this study, we tested the influence of drugs that change the actin and microtubule polymerization state on the activity and membrane expression of the PMCA transiently expressed in human embryonic kidney (HEK293) cells, which allowed us to observe and quantify these relationships in a live cell, for the first time. We found that disrupting the actin cytoskeleton with cytochalasin D significantly increased PMCA-mediated Ca^{2+} extrusion (~50–100%) whereas pre-treatment with the F-actin stabilizing agent jasplakinolide caused its full inhibition. When the microtubule network was disrupted by pretreatment of the cells with colchicine, we observed a significant decrease in PMCA activity (~40–60% inhibition) in agreement with the previously reported role of acetylated tubulin on the calcium pump. In none of these cases was there a difference in the level of expression of the pump at the cell surface, thus suggesting that the specific activity of the pump was the regulated parameter. Our results indicate that PMCA activity is profoundly affected by the polymerization state of the cortical cytoskeleton in living cells.

1. Introduction

All cells need to keep a low cytosolic free calcium concentration ($[Ca^{2+}]_{CYT} \sim 100$ nM) to maintain viability [1,2] while at the same time they use its increase as a versatile signaling pathway [3,4]. Elevations of cytoplasmic Ca^{2+} underlie a myriad of basic cellular functions ranging from extremely rapid (*e.g.* neurosecretion and skeletal muscle contraction) to long-term responses (*e.g.* cellular differentiation and mitogenesis). One of the mechanisms responsible for the maintenance of the steep Ca^{2+} concentration gradient across the plasma membrane is the plasma membrane calcium pump (PMCA) that actively expels Ca^{2+} from all eukaryotic cells with high transport affinity and selectivity [5,6]. As is widely accepted nowadays, PMCAs are able not only to maintain the long term resting Ca^{2+} levels [7] but also are key players in determining the duration and amplitude of the increase in $[Ca^{2+}]_{CYT}$ achieved after various cellular stimuli [8–10]. In order to be fully integrated in both global and local signaling events, PMCAs interact with other proteins and lipids [10] that regulate PMCA activity directly or alter the subcellular localization of the pumps. Calmodulin [11,12] and acidic phospholipids [13,14] are among the best characterized modulators of PMCA activity.

Our group discovered a novel regulatory mechanism of PMCA

Abbreviations: PMCA, plasma membrane calcium ATPase; (SERCA), (sarco)endoplasmic reticulum calcium ATPase; (HEK298 cells), human embryonic kidney 298 cells; (CytD), cytochalasin D; (JAS), jasplakinolide; (Col), colchicine; (TG), thapsigargin; (SOC), store operated channel; (SOCE), store-operated Ca^{2+} entry; (ER), endoplasmic reticulum; (AUC), area under the curve

* Correspondence to: M.G. Dalghi, Renal-Electrolyte Division, School of Medicine, University of Pittsburgh, 982 Scaife Hall, 3550 Terrace St., Pittsburgh, PA 15261, USA.
** Corresponding author.
E-mail addresses: mgd29@pitt.edu (M.G. Dalghi), jprossi@retina.ar (J.P. Rossi).

http://dx.doi.org/10.1016/j.bbamcr.2017.05.014
Received 12 January 2017; Received in revised form 11 May 2017; Accepted 15 May 2017
Available online 17 May 2017

activity that involves the actin cytoskeleton [15,16]. Actin is an abundant component of the cortical cytoskeleton and its reorganization in response to various stimuli is important in many cellular processes among which regulation of ion transport has been well established [17]. We have previously shown that purified actin can directly bind to hPMCA4b (a major human PMCA isoform) isolated from red blood cells and exert a dual modulation action on PMCA Ca^{2+}-ATPase activity: on one side F-actin inhibits PMCA [15] while short actin oligomers may be responsible for PMCA activation [16]. The latter involves an increase in the apparent affinity for Ca^{2+} and in the levels and turnover of the phosphorylated states of the pump. Due to the nature of the biophysical and biochemical approaches used, these studies had to be performed using isolated, purified proteins. However, in order to assess whether the functional interaction between the PMCA and the actin cytoskeleton may be of physiological relevance, we decided to further characterize this in the context of a living cell by monitoring in real-time the changes in the $[Ca^{2+}]_{CYT}$ affected by the PMCA.

In the present study, we tested the influence of drugs that change the actin and tubulin polymerization state on the activity and membrane expression of the PMCA2 transiently expressed in human embryonic kidney (HEK) cells. Moreover, we analyzed how PMCA handled the extrusion of two different $[Ca^{2+}]_{CYT}$ pools – one coming from the endoplasmic reticulum (ER) and the other from the extracellular *milieu* – and how its activity could be regulated under these conditions. We found that independently of the Ca^{2+} source the disruption of the actin cytoskeleton with cytochalasin D (CytD) significantly increased PMCA-mediated Ca^{2+} extrusion without affecting the level of expression of the pump at the cell surface. When cells were pre-treated with the F-actin stabilizing agent jasplakinolide (JAS), PMCA activity was reduced while ruling out that the inhibition was due to a decrease in the amount of PMCA present at the plasma membrane. Colchicine (Col) treatment also reduced PMCA2 activity, in agreement with previous reports suggesting decreased PMCA-mediated Ca^{2+} extrusion upon microtubule disruption [18].

Taken together, our results indicate that PMCA activity is profoundly affected by the polymerization state of the cortical cytoskeleton in living cells.

2. Materials and methods

2.1. Materials

HEK293 cells were obtained from American Type Culture Collection (ATCC, Manassas, VA). Lipofectamine 2000 was obtained from Life Technologies (Carlsbad, CA). Cell culture medium, fetal bovine serum (FBS), and cell culture supplements were from Invitrogen (Carlsbad, CA). The calcium 5 assay kit was purchased from Molecular Devices (Sunnyvale, CA). Thapsigargin, cytochalasin D, jasplakinolide and colchicine were purchased from Sigma-Aldrich Chemie GmbH (Buchs, Switzerland). The DC Protein Assay was purchased from BioRad Laboratories (Reinach, Switzerland). PMCA ATPase monoclonal antibody (5F10) was from Thermo Scientific, anti b-actin and anti-GAPDH antibodies were from Santa Cruz Biotechnology.

2.2. Cell culture and overexpression of hPMCA2 and hPMCA4

HEK293 cells were cultured as monolayers in Dulbecco's Modified Eagle's Medium (DMEM) supplemented with 10% FBS, 10 mM HEPES, 1 mM sodium pyruvate and 0.1 mM non-essential amino acids in a humidified incubator (37 °C, 5% CO_2). Cells were transfected with pMM2-hPMCA2w/b [19] or pMM2-hPMCA4x/b [20] using Lipofectamin 2000 as described in the manufacturer's protocol. Mock cells (cells transfected with the empty vector) were cultured in parallel as control of expression and activity.

2.3. Calcium transport measured by real-time fluorescence imaging

HEK293 cells were seeded on poly-D-lysine-coated 96-well black-walled, clear-bottom plates (Corning Costar) at a density of 1.5×10^4 cells/well. After 15 h, they were transfected with mock, PMCA2 or PMCA4 plasmids and calcium transport was assayed 24 h after transfection. Cells were loaded with calcium 5 dye (Molecular Devices) in Krebs-Ringer buffer as described previously [21] with the exception that sodium chloride was replaced by *N*-methyl-D-glucamine in order to minimize the effect of the Ca^{2+}/Na^+ exchanger. Briefly, the growth medium was removed and 100 μL dye loading buffer was added to each well and incubated for 1 h at 37 °C. Plates were not washed after dye loading. Fluorescence measurements were carried out using a fluorometric imaging plate reader ($FLIPR^{TETRA}$, Molecular Devices). Cells were excited using a 470- to 495-nm LED module, and the emitted fluorescence signal was filtered using a 515- to 575-nm emission filter for detection. Fluorescence signals were analyzed using the $FLIPR^{TETRA}$ software (ScreenWorks 3.1.2.002). PMCA-mediated Ca^{2+} efflux activity was continuously measured as follows. First, a stable baseline was established for 50 s. Thereafter, 50 μL of Krebs-Ringer buffer containing 3 × TG (1 μM final concentration unless otherwise stated) was added. After 15 min (or shorter times for CytD experiments), 50 μL of Krebs-Ringer buffer containing 4 × Ca^{2+} (1 mM final concentration unless otherwise stated) was added. In CytD, JAS and Col experiments, the corresponding compound was added to the dye solution at the desired concentration when incubation times were longer than 10 min and also added to the TG and Ca^{2+} solutions to maintain the final concentration during all the measurements. When pre-treatment consisted of 5–10 min of incubation, the drug was added together with TG at a 3 × concentration and further supplemented in the Ca^{2+} solution. To evaluate the direct effect of the compounds on the PMCA, the drug was added together with Ca^{2+} at a 4 × concentration. Traces showing the time course of fluorescence intensity were normalized to the baseline and expressed as relative cytosolic calcium ($[Ca^{2+}]_{CYT}$). Results are given as the mean ± S.E.M. from three independent experiments, each condition performed on 6 wells. Wells were excluded prior to data analysis based on poor or uneven dye loading (five to six wells in total). PMCA-mediated Ca^{2+} efflux activity was estimated using the integral of the rise in $[Ca^{2+}]_{CYT}$ from the moment of the addition of the compound (TG or Ca^{2+}) until basal levels were reached (TG) or the end of the measurements (Ca^{2+}).

2.4. Cell surface biotinylation and Western blotting

HEK293 cells were seeded on a 6-well plate at a cell density of 4.5×10^5 cells/well and maintained in supplemented DMEM as described above. After 15 h, they were transfected with mock or PMCA plasmids and plasma membrane and total expression was assayed after 24 h post-transfection. Surface proteins were biotinylated with 200 mg/mL EZ-Link Sulfo-NHS-SS-Biotin (Pierce, Reinach, Switzerland) according to the manufacturer's protocol. Cells were lysed in RIPA lysis buffer (150 mM NaCl, 50 mM Tris pH 7.4, 5 mM EDTA, 1% Triton X-100, 0.5% sodium deoxycholate, 0.1% sodium dodecyl sulfate) supplemented with protease inhibitors (Roche Applied Science), and biotinylated surface proteins were isolated using streptavidin agarose beads. Protein content in the lysate was determined using the DC protein assay (BioRad). The plasma membrane, the total lysate, and the cytosolic fraction were incubated for 2 h at room temperature with 2 × Lämmli buffer. Samples were separated using a 8% SDS gel (5 μg of protein per lane) and proteins were transferred to a PVDF blot membrane (Millipore). After blocking, the blot was incubated with the pan-PMCA primary mouse monoclonal antibody 5F10 (1:1000 dilution; Pierce) overnight at 4 °C. Goat horseradish peroxidase (HRP)–conjugated anti-mouse (1:3000; BioRad) was used as the secondary antibody. Immunoreactive bands were visualized using the enhanced chemiluminescence (ECL) method. Digital images were

quantified using GelPro Analyzer version 4.0. Protein density was normalized to the β-actin (1:1000; Santa Cruz Biotechnologies) or GAPDH (1:1000; Santa Cruz Biotechnologies) loading control.

2.5. Measurement of Ca^{2+}-ATPase activity

ATPase activity of purified PMCA, obtained as described in detail in Dalghi et al. [16], was measured at 37 °C by following the release of P_i from ATP as described previously [22]. The incubation medium was 120 mM KCl, 30 mM MOPS-K (pH 7.4), 3.75 mM $MgCl_2$, 70 μg/mL $C_{12}E_{10}$, 10 μg/mL phosphatidylcholine, 1 mM EGTA, and enough $CaCl_2$ to give the desired final free Ca^{2+} concentration. The reaction was started by the addition of ATP (final concentration 2 mM). Release of P_i was estimated using the procedure of Fiske and Subbarow [23]. Unspecific (non-enzymatic) ATP hydrolysis, determined in the absence of free Ca^{2+}, was subtracted from each measurement value. Pre-incubation with either drug or vehicle was performed as described in the figures. Measurements were performed in a Jasco V-630 Bio spectrophotometer.

2.6. Statistics

Data were expressed as mean ± S.D. from at least three independent experiments. One-way analysis of variance (ANOVA) followed by Bonferroni test was performed using GraphPad Prism version 5.00 for Windows, GraphPad Software (San Diego, CA, USA). A probability (P) value < 0.05 was considered statistically significant. Theoretical equations were fitted to the results by nonlinear regression based on the Gauss-Newton algorithm using the commercial software Sigma-Plot 12.0 for Windows.

3. Results

3.1. Characterization of $[Ca^{2+}]_{CYT}$ transients in HEK293 cells overexpressing hPMCA2 and hPMCA4

To explore how changes in the actin cytoskeleton dynamics affect the activity of PMCA in a living cell and whether this response changes under different incoming Ca^{2+} signals, we first examined the effect of the pump on Ca^{2+} transients generated by (i) Ca^{2+} released from intracellular stores, and by (ii) extracellular Ca^{2+} entry through store-operated calcium channels (SOCs). This is of interest because several downstream pathways are differentially regulated depending on the Ca^{2+} source [24–27]. To release the ER Ca^{2+} pool into the cytoplasm we added TG under nominally Ca^{2+}-free conditions. TG specifically inhibits the sarco(endo)plasmic reticulum Ca^{2+}-ATPase (SERCA) which prevents the re-uptake of Ca^{2+} back into the ER [28,29], allowing Ca^{2+} to leak out passively by yet ill-defined channels present in the ER membrane [30,31]. In Fig. 1A, a typical time course experiment is shown, which comprises a first phase involving the transient elevation in $[Ca^{2+}]_{CYT}$ upon the addition of 1 μM TG and a second phase subsequent to the addition of 1 mM Ca^{2+} to the external medium that induced a sustained $[Ca^{2+}]_{CYT}$ increase indicative of SOC activity. HEK293 cells have been widely used to investigate the mechanism of store-operated Ca^{2+} entry (SOCE) and it has been shown that they endogenously express all the components of this system, *e.g.* four TRPC, three Orai and two STIM mRNAs were found in HEK293 cells [32,33]. The magnitude of the responses obtained – a peak in $[Ca^{2+}]_{CYT}$ of ~2 fold above the basal level after the addition of TG and peaks in $[Ca^{2+}]_{CYT}$ of ~5–7 fold after the subsequent addition of 1 mM Ca^{2+} – is in complete agreement with the range of values reported for the endogenous SOCE system in HEK293 cells [32]. We confirmed an optimal TG concentration was used by determining the initial velocity of Ca^{2+} released from the ER into the cytoplasm (Fig. 1 B and C), which constitutes an indirect measurement of SERCA inhibition and ER depletion. A Hill equation is the best fit to the experimental data with a $K_{0.5}$ = (374 ± 7) nM. We also examined the TG effect on the initial velocity of the extracellular Ca^{2+} entry to determine the optimal TG condition for coupling the ER depletion to the SOC activity (Fig. 1 B and D). In this case, the initial velocity of Ca^{2+} entry was better described by a hyperbola with a $K_{0.5}$ = (78 ± 39) nM. Based on these results we decided to perform future experiments using 1 μM TG which shows saturating effects for ER depletion and SOC activation, being in full agreement with the range in which TG is generally used in cell culture and in HEK293 cells in particular [34].

We next tested the response of HEK293 cells to different $[Ca^{2+}]_{ext.}$ after pretreatment with 1 μM TG (Fig. 1E–G). The initial velocity of calcium entrance, calculated as the slope of the fluorescent signal as a function of time during the first 30s after injection, and the total calcium entry, calculated as the AUC for the interval between the addition of Ca^{2+} until the end of the measurements, showed a hyperbolic relationship with the nominal $[Ca^{2+}]_{ext.}$, displaying a $K_{0.5}$ of 1.69 ± 0.49 and 1.17 ± 0.19 mM, respectively.

Following Ca^{2+} entry, either from the ER or the extracellular medium, there is a recovery phase where Ca^{2+} is exported back out of the cell by the Na^+/Ca^{2+} exchanger and the PMCA, sequestered back in the ER by the action of the SERCA pumps and into the mitochondria, and chelated by cytosolic proteins [4]. All these events allow for restoring the basal levels of $[Ca^{2+}]_{CYT}$ after a given stimulus. In our model system (Fig. 1A), we observed that $[Ca^{2+}]_{CYT}$ returned to a level approaching the baseline after ER depletion. However, the constant Ca^{2+} influx from the extracellular medium, due to the fact that we did not wash out Ca^{2+} or add any Ca^{2+} chelating agent, could only be in part counteracted by the Ca^{2+} removal systems and a new steady state in $[Ca^{2+}]_{CYT}$ was achieved. To assess how changes in actin dynamics specifically affect PMCA activity and considering the lack of specific inhibitors for the pump, we decided to employ an overexpression approach which would also provide us with the possibility of studying different PMCA isoforms. Because PMCA isoforms exhibit different kinetic and regulatory properties, we decided to study two distinct isoforms of the pump: PMCA4, which we previously reported to be regulated by actin when studied in an isolated system [15], and PMCA2, an isoform characterized by its high basal activity and sensitivity to calmodulin [35]. We first assessed how the overexpression of both PMCA isoforms affected the shape of the Ca^{2+} signals (Fig. 2A–C). Equimolar concentrations of *N*-methylglucamine in place of NaCl were used to block the Na^+/Ca^{2+} exchanger, and TG, which blocks SERCA, was added to enhance the role of PMCA in Ca^{2+} extrusion. Because the activity of PMCA is intrinsically Ca^{2+}-dependent, comparisons were made only among conditions in which $[Ca^{2+}]_{CYT}$ signals at the beginning of the Ca^{2+} extrusion time course were in the same range. Overexpression of hPMCA2w/b (from now on named PMCA2) in HEK293 cells led to a significant decrease in the global $[Ca^{2+}]_{CYT}$ at all times after a stimulus, typically characterized by a decrease in the maximum $[Ca^{2+}]_{CYT}$ reached (*i.e.*, the amplitude of the Ca^{2+} signal), a slight shift to the left in the time at which this maximal concentration is achieved and a reduced plateau value in the sustained Ca^{2+} entry phase mediated by SOCs. For further comparisons, quantification of the effect of PMCA overexpression and the corresponding treatments was done based on the area under the curve (AUC) comprised as follows: (i) for the first phase, from the time of addition of TG until the time when $[Ca^{2+}]_{CYT}$ returns to the baseline and (ii) for the second phase, from the time after addition of Ca^{2+} until the end of the experimental recordings. The AUC thus represents the overall $[Ca^{2+}]_{CYT}$ of each phase, such that a more effective mechanism of Ca^{2+} extrusion will be reflected in an overall AUC decrease. PMCA2 overexpression reduced the increase in $[Ca^{2+}]_{CYT}$ induced by TG by 57 ± 7% and that mediated by SOCs by 31 ± 7% compared to mock-transfected cells. Unexpectedly, overexpression of hPMCA4x/b resulted in no significant difference in $[Ca^{2+}]_{CYT}$ handling compared to mock-transfected cells for any of the stimuli in spite of being successfully overexpressed (data not shown). As seems to be true for all eukaryotic

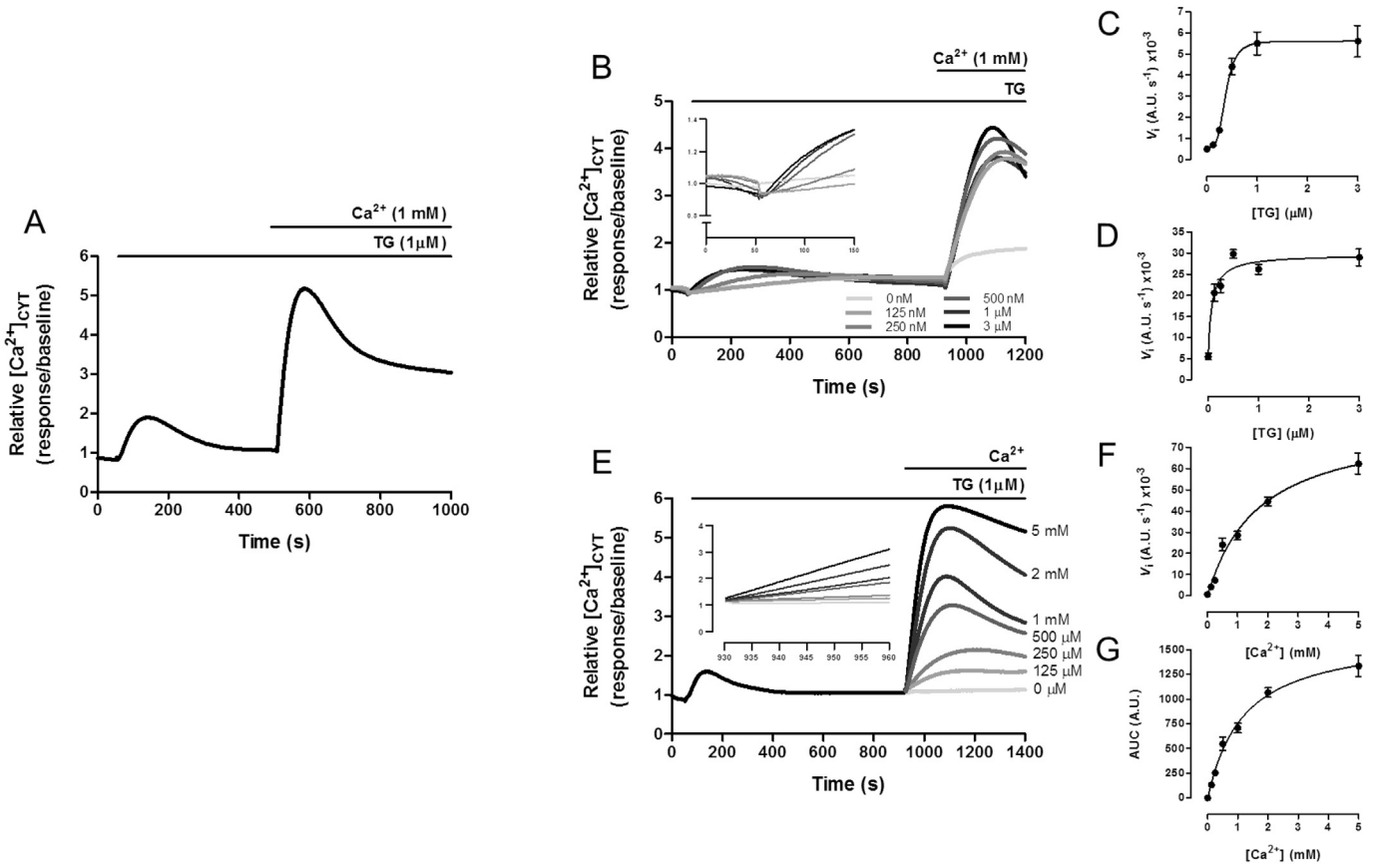

Fig. 1. Pattern of Ca^{2+} transients in HEK293 cells induced by TG and SOCs. (A) Representative traces of the time course of $[Ca^{2+}]_{CYT}$ in HEK293 cells upon addition of 1 μM TG in nominal free Ca^{2+} medium and after adding Ca^{2+} (1 mM) to the extracellular solution. (B) Dependence of $[Ca^{2+}]_{CYT}$ transients on the TG concentration (0–3 μM) at a fixed extracellular Ca^{2+} concentration (1 mM). *Inset*: Detail of the Ca^{2+} signal obtained in the time range of 0–100 s after TG addition. (C) Initial velocity of Ca^{2+} released from the ER after TG addition as a function of TG concentration calculated as the first derivate of the Ca^{2+} signal as a function of time from data shown in (A-*inset*). (D) Initial velocity of Ca^{2+} entry from the extracellular medium after Ca^{2+} addition to the medium as a function of TG concentration calculated as the first derivate of the Ca^{2+} signal as a function of time from data shown in (A). (E) Dependence of $[Ca^{2+}]_{CYT}$ transients on the extracellular Ca^{2+} concentration (0–5 mM) at a fixed, saturating concentration of TG (1 μM). *Inset*: Detail of the Ca^{2+} signal obtained during the first 30s after Ca^{2+} addition. (F) Initial velocity of Ca^{2+} entry from the extracellular medium after Ca^{2+} addition to the solution as a function of the extracellular Ca^{2+} concentration calculated as the first derivate of the Ca^{2+} signal as a function of time from data shown in (E). (G) Area under the curve of the $[Ca^{2+}]_{CYT}$ signal as a function of the extracellular Ca^{2+} concentration calculated as the integral of the signal in the time range from the addition of Ca^{2+} to the end of the recordings. All experiments were performed in $n = 6$ in 2–3 independent experiments.

cells, HEK293 cells express endogenous PMCAs, as illustrated in Figs. 3G, 4F and 5E. The antibody we used in these experiments (5F10, Thermo Scientific) does distinguish between the four isoforms of the pump, but it has been previously reported that the isoforms present in HEK293 cells are PMCA1b and PMCA4b [34–37]. Previous studies in HeLa cells have shown that the abundance of PMCA4 only moderately influences the SOC Ca^{2+} signal [37]. This is in agreement with our finding that overexpression of PMCA4, which was 5 to 7 times above the endogenous PMCA levels in the transfected HEK293 cells, had little impact on the $[Ca^{2+}]_{CYT}$ transients. One possible explanation is that much of the overexpressed PMCA4 is functionally "silent" because of a lack of trafficking and integration in the plasma membrane. In HeLa and Huvec cells the delivery of PMCA4b to the plasma membrane is strongly enhanced when the cells reach confluence [37,38]; in our transient expression system the amount of PMCA4b actually present in the cell membrane may thus be limited. It has also been shown that PMCA4b is inhibited by the SOC components STIM1/Orai upon sustained store-operated Ca^{2+} entry [39], which may further help to explain why overexpression of PMCA4b showed little or no effect on $[Ca^{2+}]_{CYT}$ transients in our system. In contrast, PMCA2 shows very different characteristics and accordingly, its overexpression (by 7.6 ± 1.8 fold in total lysates and 11.0 ± 0.3 fold in membranes) significantly enhanced Ca^{2+} extrusion, probably due to its fast kinetics [37]. Based on these findings, we decided to continue our study on the regulation of PMCA by the actin cytoskeleton using PMCA2 as a model.

3.2. Depolymerization of the actin cytoskeleton by Cytochalasin D stimulates Ca^{2+} efflux mediated by hPMCA2

To test the hypothesis that the activity of the PMCA can be increased by shortening the actin filaments present in living cells, we used cytochalasin D (CytD), a fungal metabolite that induces gradual depolymerization of actin by binding to the fast-growing barbed end of the filaments [40,41]. Due to its membrane-permeant property, CytD is suitable to induce filament disruption in intact cells. The experimental procedure consisted in pre-incubating the cells with DMSO (vehicle control) or CytD for the period of time indicated in each figure, followed by the addition of 1 mM Ca^{2+} to the extracellular medium once the $[Ca^{2+}]_{CYT}$ reached plateau values after the first transient induced by 1 μM TG treatment in nominally Ca^{2+}-free medium. In this way, we sought to determine whether a rise in $[Ca^{2+}]_{CYT}$ originating from different sources differently impacts the response of the pump upon CytD treatment. Compared to TG-evoked Ca^{2+} transients, the Ca^{2+} signal mediated by SOCs represents not only a different mechanism of Ca^{2+} entry into the cytosol but also a much higher increase in its level as discussed in the previous section. The value of the AUC (calculated as described under Materials and methods) obtained for mock-transfected HEK293-cells treated with vehicle was established as

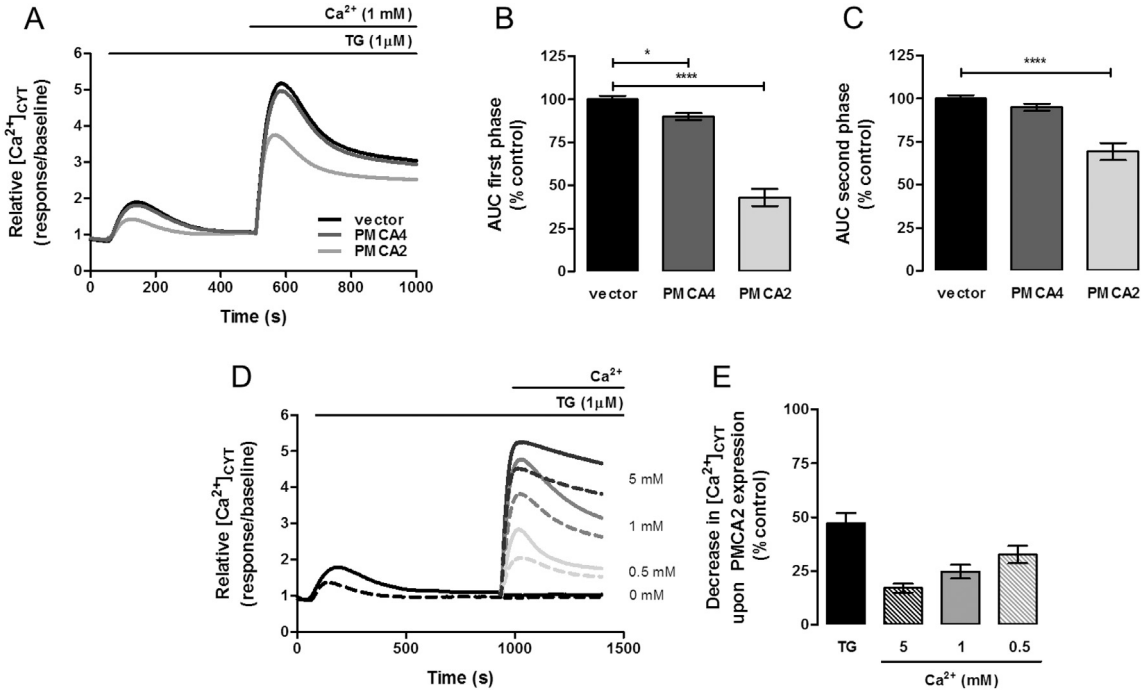

Fig. 2. Effect of PMCA4 and PMCA2 overexpression on the shape of the Ca^{2+} transients in HEK293 cells induced by TG and SOCs. (A) Representative traces of the time course of $[Ca^{2+}]_{CYT}$ in HEK293 cells transiently overexpressing PMCA4 or PMCA2 or transfected with empty vector (control) upon addition of 1 μM TG in nominal free Ca^{2+} medium and after adding Ca^{2+} (1 mM) to the extracellular solution. (B) Area under the curve of the $[Ca^{2+}]_{CYT}$ signal after TG (1 μM) addition (first phase). Significant differences from control are indicated as $*p < 0.05$ and $****p < 0.0001$ (one-way ANOVA). (C) Area under the curve of the $[Ca^{2+}]_{CYT}$ signal after addition of Ca^{2+} to the extracellular solution (1 mM; second phase). AUC were calculated as indicated under Materials and methods, significant differences from control are indicated as $****p < 0.0001$ (one-way ANOVA). (D) Representative traces of the time course of $[Ca^{2+}]_{CYT}$ in HEK293 cells transiently overexpressing PMCA2 (dashed curve) or transfected with empty vector (bold curve) upon addition of 1 μM TG in nominal free Ca^{2+} medium and after adding different Ca^{2+} concentrations to the extracellular solution. (E) Effect of PMCA2 expression in Ca^{2+} removal from the cytosol after TG or TG plus extracellular Ca^{2+} at different concentrations as shown in (D) expressed as the percentage of AUC with respect to mock transfected HEK293 cells at each given TG or TG-Ca^{2+} concentration. All experiments were performed in $n = 6$ in 2–3 independent experiments.

100% and values of AUC obtained for all other conditions were related to this reference value. By performing ANOVA analysis on these data, we assessed whether the treatment affected the behavior of the mock-transfected HEK293 cells, the effect of PMCA2 overexpression, and the effect of the treatment on PMCA2 function. To quantify the latter, we considered the difference in AUC between mock-transfected HEK293 cells and HEK293-PMCA2 cells treated with vehicle as the activity of PMCA2 under control conditions. We then calculated the difference in AUC between mock-transfected HEK293 cells and HEK293-PMCA2 cells treated as described for each experiment and related to the control as described in Eq. (1):

$$\%PMCA2activity = \frac{(AUC_{mock,treatment} - AUC_{PMCA2,treatment})}{(AUC_{mock,veh} - AUC_{PMCA2,veh})} \times 100 \quad (1)$$

Pretreatment of HEK293-PMCA2 cells with 5 μM CytD for 5 min prior to the start of the recordings resulted in a significant decrease in the AUC of the $[Ca^{2+}]_{CYT}$ signal released from the ER stores compared to vehicle treated HEK293-PMCA2 cells (Fig. 3A and B). Using Eq. (1) we obtained a value of 138 ± 13% for PMCA2 activity; the control value for PMCA2 activity was (100 ± 17) %, as summarized in Table 1. This means that Ca^{2+} extrusion mediated by PMCA2 increased ~40%. CytD showed no significant effect in mock-transfected cells compared to vehicle control, meaning that under these conditions neither the processes of Ca^{2+} release from the ER nor its removal from the cytosol are affected. This is in agreement with previous reports showing that treatment of HEK293 cells [42] or other cell types [43,44] with different actin filament disrupting agents does not affect the Ca^{2+} transients evoked by TG. However, there are divergent findings regarding the role for actin cytoskeleton breakdown in the coupling of store depletion to the activation of SOCs, ranging from no observed effect [44,45] to inhibition [46] or increased activation in SOC activity [42]. This apparent discrepancy may be attributed to a cell type dependent differential contribution of the cytoskeleton to the SOC activity [43]. The role of CytD was then assessed only under conditions where a minimal effect in SOCs activity was observed, as in HEK293 cells an increase in SOC activity was reported to occur upon actin depolymerization [42].

To trigger the second phase of the experiments shown in Fig. 3A, Ca^{2+} was added 10 min after the start of the recordings, which represents an overall 15 min pre-incubation of the cells with CytD. Under these conditions, we observed no effect of CytD in mock transfected HEK293 cells, but a significant increase in Ca^{2+} removal from the cytosol in HEK293-PMCA2 cells with respect to vehicle control (Fig. 3A and C). Calculating the change in PMCA2 activity due to CytD treatment, we obtain a ~100% increase; PMCA2 activity upon CytD treatment was 204 ± 24% compared to vehicle values of 100 ± 2%. These results suggest that CytD treatment of the cells increases PMCA2-mediated Ca^{2+} removal from both Ca^{2+} sources, the ER and the extracellular medium. Direct comparison of the magnitude of the effect between the two phases is not possible because there are two variables (i) the time of pre-incubation with CytD which is different for the start of each phase, very likely representing a different state of actin polymerization, and (ii) the extent of the Ca^{2+} transient reached. We next decided to focus on the second phase. We reasoned that changes in the extent of actin depolymerization – achieved by changes in the pre-treatment conditions with CytD – may be reflected in the levels of Ca^{2+} extrusion mediated by the pump as a consequence of a difference in the level of activation. Longer incubation times had to be avoided as they led to round-shaped cells with higher possibility of detachment from the plate surface upon injection and significant impact on SOCs activity. Therefore, we decided to pre-treat the cells for a shorter period of time during which CytD was added concomitantly with TG (Fig. 3D and E), representing a 7.5 min pre-incubation time until the addition of Ca^{2+} in the extracellular medium. Under these conditions, 5 μM CytD

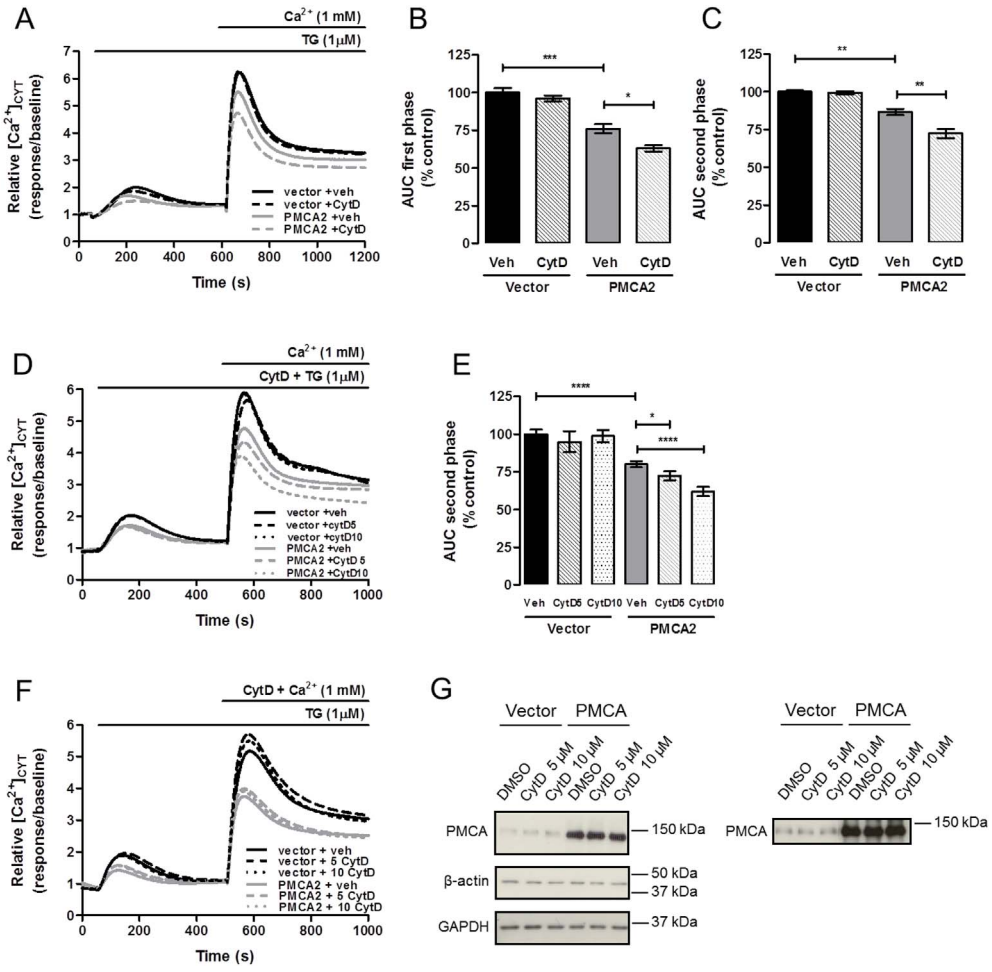

Fig. 3. Effect of Cytochalasin D on PMCA2-mediated Ca^{2+} extrusion. Representative traces of the time course of $[Ca^{2+}]_{CYT}$ in HEK293 cells transiently overexpressing PMCA2 or transfected with empty vector (control) upon addition of: (A) CytD (5 μM) 5 min prior to the start of the recordings, (D) CytD (5–10 μM) concomitant to the addition of TG, and (F) CytD (5–10 μM) concomitant to the addition of Ca^{2+} to the extracellular solution, In all cases the experimental scheme described in Fig. 2A was followed. Bar graphs show the area under the curve of the $[Ca^{2+}]_{CYT}$ signal in the experiment shown in (A) after addition of (B) TG (first phase), and (C) Ca^{2+} (second phase), and (E) of that depicted in (D) after addition of Ca^{2+}. AUC were calculated as indicated under Materials and methods, significant differences are indicated as $*p < 0.05$, $**p < 0.01$, $***p < 0.005$, $****p < 0.0001$ (one-way ANOVA). Data are from three independent experiments performed in $n = 6$. (G) Immunoblot of total PMCA protein expression in whole lysate (*left panel*) or in the plasma membrane (*right panel*) after incubation of HEK293-PMCA2 or HEK293 transfected with the empty vector with 5 and 10 μM CytD for 15 min, representative from three different experiments. For the loading control of the whole lysate, β-actin and GAPDH were assessed.

resulted in a PMCA activity of (114 ± 8) %, which represents a slight increase in PMCA activity compared to control which was (100 ± 4)%. This means that by reducing the time of incubation with CytD there was a reduction in the magnitude of the effect. When used at a higher concentration for the same period of time, CytD (10 μM) led to a greater increase in PMCA2 activity reaching a value of (185 ± 4) %. This suggests that there is a certain extent of actin depolymerization leading to PMCA2 activation which can be achieved either by changing the time or the concentration of CytD. In summary, these results suggest that CytD, most likely through its depolymerizing effect on the actin filaments, was able to induce an increase in removal of cytosolic Ca^{2+} mediated by the PMCA2. Interestingly, it has been recently reported that upon an increase in $[Ca^{2+}]_{CYT}$ there is a rapid and transient actin rearrangement involving the depolymerization of cortical actin [47]. Calcium release from ER stores was observed to be insufficient to induce a decrease in actin filaments at the cell cortex, and the presence of high extracellular calcium was needed to observe such effect [47]. This would mean, then, that under our experimental conditions, PMCA2-HEK293 cells treated with vehicle could be activated in the second phase as a consequence of the effect of calcium on the actin cytoskeleton. If this is the case, we may be underestimating the magnitude of the CytD treatment. Beyond this consideration, future studies assessing whether and how changes on actin dynamics induced by a substantial increase in $[Ca^{2+}]_{CYT}$ affects PMCA activity will be highly valuable in understanding calcium signaling pathways and homeostasis.

In order to rule out a possible direct effect of CytD on the pump, we added CytD concomitantly with the Ca^{2+} addition (Fig. 3F). We observed no effect on the AUC of the response at any of the concentrations used (5 and 10 μM) implying that a certain period of time is needed for these regulatory phenomena to occur. These findings are compatible with an effect on altering actin dynamics and unlikely a direct effect of the drug on the pump. This is also evident in Fig. 3D, where no effect of CytD can be observed in the extrusion of Ca^{2+} released from the ER (first phase of the curve) when added concomitant to TG. The time-dependency of the observed effect, in addition to the lack of immediate effect of CytD on the pump, is strong evidence in favor of a cytoskeleton-mediated effect of CytD. Based on our previous observations, we hypothesize that shortening actin filaments increases PMCA activity. To demonstrate that in a living cell system this may also be the case, we sought to rule out that the actin cytoskeleton was affecting PMCA2 trafficking to the plasma membrane. Thus, to determine whether HEK293-PMCA2 cells incubated with CytD show altered PMCA2 expression at the plasma membrane, we used membrane-impermeant sulfo-NHS SS biotin to label cell surface proteins selectively. These were then isolated with streptavidin beads, and Western

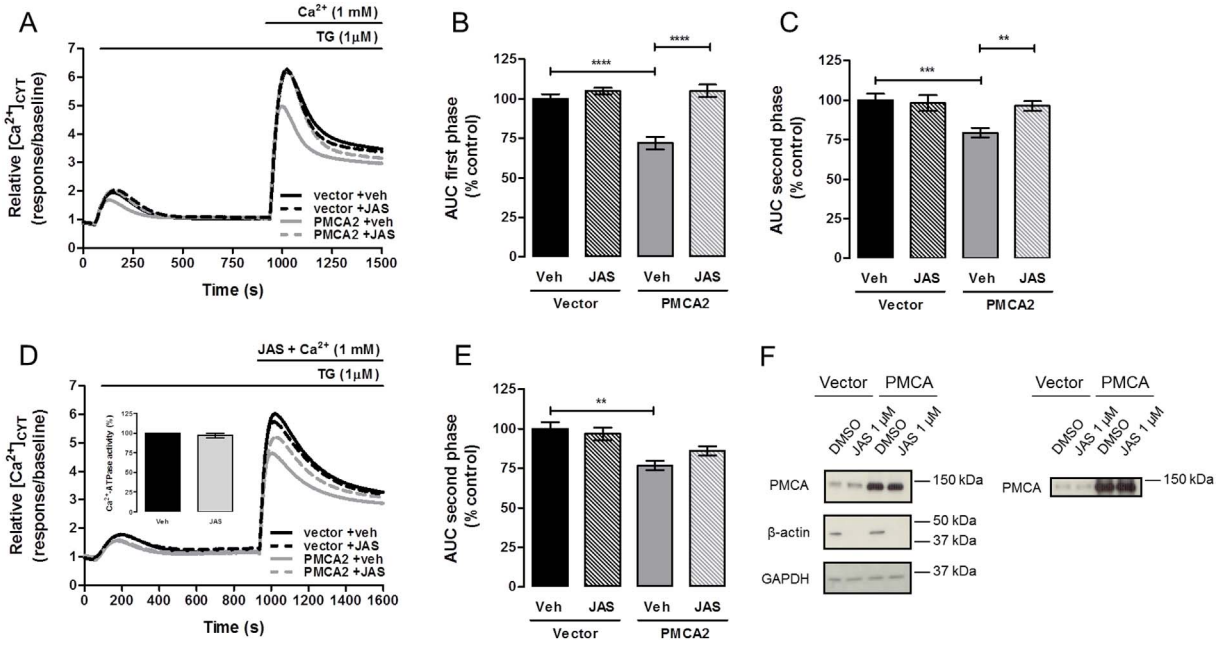

Fig. 4. Effect of Jasplakinolide on PMCA2-mediated Ca^{2+} extrusion. Representative traces of the time course of $[Ca^{2+}]_{CYT}$ in HEK293 cells transiently overexpressing PMCA2 or transfected with empty vector (control) upon addition of: (A) JAS (1 μM) for 1 h prior to the start of the recordings, and (D) JAS (1 μM) concomitant to the addition of Ca^{2+} to the extracellular solution. In all cases the experimental scheme described in Fig. 2A was followed. Area under the curve of the $[Ca^{2+}]_{CYT}$ signal in experiments shown in (A) after addition of: (B) TG (first phase), and (C) Ca^{2+} (second phase), and in (D) after the addition of (E) Ca^{2+} (second phase). AUC were calculated as indicated under Materials and methods, significant differences are indicated as $^{**}p < 0.01$, $^{***}p < 0.001$, $^{****}p < 0.0001$ (one-way ANOVA). Data are from three independent experiments performed in $n = 6$. *Inset* (D): Direct effect of JAS (1 μM, 5 min pre-incubation) assessed on purified PMCA by measuring the Ca^{2+}-ATPase activity of the pump in presence of the drug or DMSO as vehicle control (data from three independent experiments performed in triplicates). When not apparent the error bar is within the columns. (F) Immunoblot of total PMCA protein expression in whole lysate (*left panel*) or in the plasma membrane (*right panel*) after incubation of HEK293-PMCA2 or HEK293 transfected with the empty vector with 1 μM JAS for 1 h, representative from three different experiments. β-actin and GAPDH were also assessed and the latter was taken as loading control.

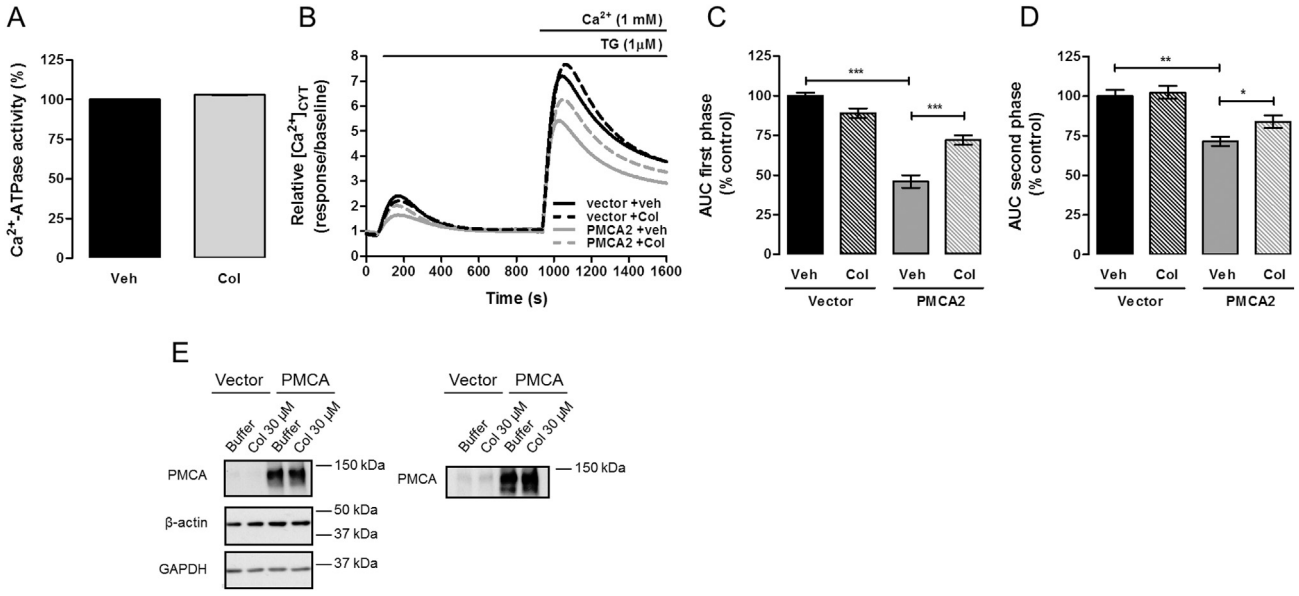

Fig. 5. Effect of Colchicine on PMCA2-mediated Ca^{2+} extrusion. (A) Direct effect of Col (30 μM, 5 min pre-incubation) was assessed on purified PMCA by measuring the Ca^{2+}-ATPase activity of the pump in presence of the drug or buffer as vehicle control. When not apparent the error bar is within the columns. (B) Representative traces of the time course of $[Ca^{2+}]_{CYT}$ in HEK293 cells transiently overexpressing PMCA2 or transfected with empty vector (control) upon pre-incubation with Col (30 μM) for 30 min prior to the start of the recordings. The experimental scheme described in Fig. 2A was followed. Area under the curve of the $[Ca^{2+}]_{CYT}$ signal in experiments shown in (B) after addition of: (C) TG (first phase), and (D) Ca^{2+} (second phase). AUC were calculated as indicated under Materials and methods, significant differences are indicated as $^{*}p < 0.05$, $^{**}p < 0.005$, $^{***}p < 0.0005$ (one-way ANOVA). Data are from three independent experiments performed in $n = 6$. (F) Immunoblot of total PMCA protein expression in whole lysate (*left panel*) or in the plasma membrane (*right panel*) after incubation of HEK293-PMCA2 or HEK293 transfected with the empty vector with 30 μM JAS for 30 min, representative from three different experiments. For the loading control of the whole lysate, β-actin and GAPDH were assessed.

blotting was used to quantify surface expression levels. The PMCA antibody (5F10) detected a band of ~140 kDa from HEK293-hPMCA2 and mock transfected cells, consistent with the pump running as a monomer under denaturing conditions. Since the treatment could affect the actin content in the supernatant of the lysate, we used both β-actin and GAPDH as loading controls. CytD treatment had no effect on the surface nor the total expression of PMCA2 (Fig. 3G), indicating that an effect on the pump trafficking is unlikely to account for the increase in

Table 1
Effect of actin depolymerization by CytD on PMCA2 activity.

Treatment	PMCA2 activity (mean ± S.E.M. in % of control)	
	First phase	Second phase
Vehicle (0.1% DMSO)	100	100
CytD 5 μM, 5 min preincubation	138 ± 8	204 ± 17
CytD 5 μM, 7.5 min preincubation (CytD + TG)	N.A.	114 ± 22
CytD 10 μM, 7.5 min preincubation (CytD + TG)	N.A.	185 ± 12
CytD 5 μM, no preincubation (CytD + Ca^{2+})	N.A.	119 ± 16
CytD 10 μM, no preincubation (CytD + Ca^{2+})	N.A.	103 ± 9

N.A.: Not applicable.

Ca^{2+} efflux in response to CytD treatment. Although relocalization of the PMCA to the plasma membrane was suggested to be regulated by the actin cytoskeleton, as treatment with CytD blocked PMCA translocation [48], we have not found experimental evidence that supports this observation. Based on these results, we propose that it is the activity of the pump that is modulated by actin filament depolymerization, and not its abundance in the plasma membrane. Whether PMCA activity regulation involves the direct interaction with actin molecules, as previously observed *in vitro,* cannot be inferred from these experimental results (see Discussion).

3.3. Stabilization of F-actin by jasplakinolide inhibits Ca^{2+} efflux mediated by hPMCA2

We have previously shown that purified PMCA4 is inhibited by F-actin [15]. This, in addition to the preceding data, made us wonder whether stabilization of the actin filament network which lies close to the plasma membrane could lead to the pump inhibition *in vivo*. With this aim, we used jasplakinolide (JAS), a cell-permeant peptide isolated from the marine sponge *Jaspis johnstoni*, that induces actin polymerization at the same time that it stabilizes pre-existing filaments [49,50] by potently binding to F-actin (K_d = 15–300 nM; [49]). Cells were pre-treated with 1 μM JAS for 1 h; these conditions were found, in our hands and by others [49], to produce the maximal detectable effects of JAS without adversely affecting gross cell shape or adherence. Under these conditions, we observed a full inhibition of Ca^{2+}-extrusion mediated by PMCA2 (Fig. 4A–C) as revealed by the overlapping traces of HEK293-PMCA2 and HEK293 treated with JAS. Quantification of JAS effects on PMCA2 is summarized in Table 2. The JAS effect was observed for both phases of the curves, meaning that actin polymerization leads to an impaired PMCA-mediated Ca^{2+} recovery when a $[Ca^{2+}]_{CYT}$ increase occurs as a consequence of either ER depletion or extracellular influx. JAS has been reported to have no significant effect on the extent of Ca^{2+} release from the ER upon TG treatment [42,44] which is in agreement with our observations. However, JAS has been reported to inhibit SOCs activity [44]. Galán et al. [42] reported a ~60% attenuation of SOCs activity in HEK293 cells. However, in this study the authors used a concentration of JAS 10 times higher than the one used in the present work and JAS effects can vary strongly in a time- and concentration-dependent manner as previously reported [50].

Table 2
Effect of actin polymerization by JAS on PMCA2 activity.

Treatment	PMCA2 activity (mean ± S.E.M. in % of control)	
	First phase	Second phase
Vehicle (0.1% DMSO)	100	100
JAS 1 μM, no preincubation (JAS + Ca^{2+})	N.A.	47 ± 32
JAS 1 μM, 1 h	9 ± 16	0

Similarly to the approach used in CytD experiments, we reasoned that if we added JAS simultaneously with Ca^{2+}, we could assess whether the drug possesses an effect independent of the one exerted on actin polymerization, which would thus most likely represent a direct effect of the compound on the pump. When we added JAS together with Ca^{2+}, we found a slight but not statistically significant inhibition of PMCA-mediated Ca^{2+} extrusion (Fig. 4D–E). We further confirmed these results by assessing the effect of JAS on PMCA isolated from human red blood cells (*Inset* in Fig. 4D) where we observed no difference in the Ca^{2+}-ATPase activity of the pump upon JAS pre-incubation (1 μM, 5 min) compared to vehicle control (DMSO).

In order to determine whether inhibition of Ca^{2+} extrusion mediated by PMCA2 could be attributable to a reduction in PMCA2 expression at the plasma membrane, we performed biotinylation assays as described in the previous section. We did not observe any difference in PMCA2 expression in the plasma membrane, nor in the total amount, when cells were pre-treated with JAS, under the same conditions as those used in the functional assays, compared to vehicle. Similarly to what we did in the CytD experiments, we used β-actin and GAPDH as loading controls. In this case, we did observe a difference in the amount of β-actin present in the samples: β-actin was completely absent when the cells were pre-treated with JAS (1 μM, 1 h, 37 °C). This is due to the centrifugation step following cell lysis which allows for a clear supernatant depleted from cell debris. The large F-actin aggregates formed upon JAS treatment very likely remained in the pellet fraction. Indeed, this is the principle of a widely used biochemical method as well as commercial kits developed to study the ratio between G- and F-actin [51]. In this case we took advantage of this phenomena to show that JAS is effectively enhancing F-actin content and used GAPDH as the loading control. However, we did not observe any difference in β-actin content in the samples treated with CytD (compared to vehicle control, DMSO; see Fig. 3G). This may be explained by the fact that this method uses high centrifugation speed (typically 100,000 × *g*, 1 h), unlike the conditions we used to clear the lysate (350 × *g*, 5 min) under which only big clusters of F-actin aggregates sediment.

Taken together, these data indicate that a shift from G-actin or shorter filaments towards F-actin inhibits PMCA activity without showing an effect on its expression in the plasma membrane.

3.4. Depolymerization of microtubules by colchicine decreases Ca^{2+} efflux mediated by hPMCA2

It has been previously shown that tubulin binds to PMCA and inhibits its enzyme activity [18]. In this study, Monesterolo et al. [18], investigated the effect of acetylated tubulin on PMCA activity in vesicles isolated from brain synaptosomes, where they found that taxol, a known microtubule stabilizing agent, led to a decrease in the amount of acetylated tubulin/PMCA complex and stimulated PMCA activity. Nocodazole, an inhibitor of tubulin polymerization, showed a strong inhibitory effect (~80% of inhibition) in spite of also promoting the dissociation of the complex. The authors showed that the inhibition could be explained by a direct effect of the drug on the pump. However, the effect of microtubule depolymerization on PMCA activity and its impact in the context of a living cell remains to be addressed. To this aim, we treated HEK293-PMCA2 cells with colchicine (Col), another microtubule depolymerizing agent [52–54] that showed no direct effect on PMCA2 activity (Fig. 5A). We observed that Col (30 μM, 30 min) led to a significant increase in the AUC of the $[Ca^{2+}]_{CYT}$ signal both after Ca^{2+} release from the ER stores and after Ca^{2+} influx from the extracellular medium (Fig. 5B–D): PMCA2-mediated Ca^{2+} extrusion showed ~70% and ~60% of inhibition for the first and second phases, respectively (Table 3). As was also shown for the actin cytoskeleton,

Table 3
Effect of microtubule depolymerization by Col on PMCA2 activity.

Treatment	PMCA2 activity (mean ± S.E.M. in % of control)	
	First phase	Second phase
Vehicle (0.1% DMSO)	100	100
Col 30 μM, 30 min	31 ± 6	64 ± 14

several studies have reported that depolymerization of the microtubular cytoskeleton using nocodazole did not affect SOCs currents [44,55], while others have shown that nocodazole and, to a lesser but still significant extent colchicine (100 μM, 20 min) could decrease SOC-mediated Ca^{2+} influx [56]. Moreover, it has also been observed that treatment with colchicine enhanced the activation of SOCs by ER depletion [42]. Under our experimental conditions (30 μM, 30 min), we observed no significant effect of colchicine on ER- or SOC-mediated calcium transients.

In order to rule out that a reduction in PMCA2 expression at the plasma membrane could account for the decrease in Ca^{2+} extrusion we again performed biotinylation assays. We did not observe any difference in PMCA2 expression in the plasma membrane, nor in the total lysate amount, when cells were pre-treated with Col under the same conditions as those used in the functional assays. This was the expected result given the previous observations on the effect of tubulin on the catalytic activity, but not in the trafficking, of the pump. Our interpretation for the inhibitory effect of Col on PMCA2 activity is that the promotion of microtubules depolymerization leads to a rise in the tubulin (the dimer) pool in the cell, which in turn forms a complex with the pump to inhibit its activity. The same reasoning would explain the previously reported effect of taxol [18]: reducing the "free" tubulin pool by assembling tubulin into the microtubule would lead to a decrease in tubulin/PMCA complex by the law of mass action, releasing the pump from inhibition. However, it has not yet been fully demonstrated, and is beyond of the scope of the present study, whether the (acetylated) tubulin species that forms a complex with the enzyme is a constituent of microtubules or an isolated tubulin dimer. Our results, and the previously reported taxol experiments, would support the latter.

4. Discussion

We previously reported a novel regulatory mechanism of PMCA activity by actin using an *in vitro* system [15,16], showing that actin differentially regulates the pump's catalytic activity depending on its polymerization state. We found that both, G- and F-actin bind directly to the pump and induce conformational changes that may help explain the effects observed on the activity of PMCA. Short actin oligomers – consisting of 3–4 actin monomers – have been observed to produce the maximal activation of the pump [16]. Interestingly, short filamentous actin has been observed at or close to the plasma membrane [57,58]. Moreover, it has been recently shown that a rise in $[Ca^{2+}]_{CYT}$ leads to rapid and transient actin rearrangements, consisting in filament polymerization around the nucleus and at the ER, while cortical actin is being disassembled [47,59]. Actin depolymerization upon calcium increase in the micromolar range had been shown to be promoted through pathways involving gelsolin, villin and cofilin [60–62]. These observations further suggest that a regulatory mechanism of PMCA activity comprised by differential actin dynamics at the cell cortex may well be of physiological relevance. With this aim, we tested the effect of altering the actin cytoskeleton dynamics in a living cell while monitoring in real-time the changes in Ca^{2+} transients. We found that PMCA2 is able to shape the Ca^{2+} transients arising from both the ER and the extracellular environment under control conditions, in agreement with Pászty et al. [37]. When HEK293 overexpressing PMCA2 were incubated with CytD, we found that PMCA-mediated Ca^{2+} extrusion increased in a time- and concentration-related manner. This, in addition to (i) the lack of an immediate effect of the drug in the cells, (ii) the lack of a direct effect of CytD on the pump, previously reported on purified PMCA [58], and (iii) the lack of an effect on the total and membrane expression of PMCA2, led us to suggest that CytD-mediated actin depolymerization increases PMCA2 specific activity. We thus hypothesize that, similar to the activation of the pump by the calcium-calmodulin system, actin can act as a sensor of the $[Ca^{2+}]_{CYT}$ resulting in the formation of actin species – *i.e.* short oligomers – that lead to PMCA activation which in turn results in the restoration of the normal low $[Ca^{2+}]_{CYT}$. It is interesting to note that calcium released from the ER was shown to be insufficient to promote actin rearrangements in several cell lines and extracellular calcium influx was required [47]. If this is the case, we expect that PMCA becomes activated by actin depolymerization only under circumstances where a relatively high and sustained Ca^{2+} influx from the extracellular medium is involved. Further studies will be required to address under which types of Ca^{2+} signaling events the pump is activated by this mechanism; this will involve the correlation between how an increase in $[Ca^{2+}]_{CYT}$ modifies actin dynamics at the cell edge – ER released *versus* extracellular influx – and how this impacts PMCA activity. During T cell activation, where a rapid release of Ca^{2+} from the ER is followed by a sustained influx of extracellular Ca^{2+} across the plasma membrane via SOCs, actin undergoes rapid rearrangements, which in turn induce feedback regulation of Ca^{2+} signaling [63]. Thus, if actin depolymerization is able to increase PMCA activity, PMCA could be one of the key pieces in the reciprocal interdependence previously described between Ca^{2+} signaling and cytoskeletal rearrangements [63].

In addition to our observation on the effect of actin depolymerization on PMCA activity, the opposite situation also appeared to be true: when actin polymerization was induced using JAS, Ca^{2+} extrusion mediated by PMCA2 was completely abolished. In this case again, the direct effect of the drug on the pump as well as changes in the total expression or in the trafficking of the pump towards the plasma membrane were ruled out. Together, these results suggest that actin dynamics plays a role in regulating PMCA activity in intact cells.

Our previous *in vitro* studies showed that actin regulates PMCA activity by a direct interaction with the pump, as described at the beginning of this section. However, there are many possible explanations that may account for the observed effect in a living cell system other than or in addition to a direct interaction between the PMCA and the actin molecules. Padányi et al. (2009) [64] showed that depolymerization of the actin cytoskeleton by cytochalasin D increased PMCA4b cluster areas, attributing actin a role of fence able to limit the lateral diffusion of the pump. However, they did not address if or how this affected the pump's activity. One possible mechanism for the observed effect of cytoskeleton rearrangement is a differential mobility of the pump within the plasma membrane, which may affect its translation in or out of certain regions (*e.g.* lipid rafts) where its activity can be differentially regulated by a new lipid environment, other binding partners or by changing its oligomeric state [65–67]. Oligomeric PMCA appears to be present in caveolae where the pump molecules are 18- to 25-fold concentrated compared to non-caveolae regions [65–67] and where the biologically most relevant PMCA activators, acidic phospholipids and calmodulin, are enriched [68,69]. Interestingly, PIP_2 – an acidic phospholipid that increases PMCA activity [14,70] and – which is itself promoted by an increase in Ca^{2+} – is also a critical regulator of actin dynamics [71]. Clearly, the interrelationship between Ca^{2+}, PMCA and actin is extremely complex as may be also true for the other major substrate of the pump, ATP. Thus, another possible explanation for PMCA regulation by actin may be the differential accessibility and/or availability of substrates, *i.e.* Ca^{2+} and ATP. Actin causes an increase in the medium viscosity when polymerized which might be relevant to explaining why F-actin inhibits PMCA activity. Previous studies from our laboratory [15,72] using human erythrocyte membranes suggest that accessibility of the sub-

strates (Ca^{2+} and ATP) is not the cause of the observed decrease in PMCA activity. However, it would be very interesting to assess whether actin filaments or microtubule dynamics can affect the ATP levels in the surroundings of the pump in a living cell. Actin requires ATP for polymerization, hence ATP depletion could be expected in areas of high actin turnover and net actin assembly. Suzuki et al. (2015) [73] showed that cells treated with Latrunculin A – which binds with 1:1 stoichiometry to monomeric actin, sequestering monomers and preventing their assembly – had increased ATP levels at the edge of the cell. Potentially, then, the increase in actin polymerization due to the jasplakinolide treatment may inhibit PMCA activity by decreasing ATP levels. Future studies using ATP sensors in living cells [74] may be able to address this hypothesis. Alternatively, actin polymerization could impair the accessibility of PMCA to cytosolic modulators (*i.e.* calmodulin). It would be interesting to determine if changes in the actin cytoskeleton dynamics modify the pump interactome profile. This would provide valuable information about the calmodulin accessibility to the C-terminal tail of the pump as well as changes in the interaction of the pump with other known binding partners. Such changes may influence not only PMCA activity but also the coupling of the pump to these proteins, thereby affecting the signaling pathways in which they are involved.

The involvement of the actin cytoskeleton in modulating PMCA activity is not exclusive but has been observed in other transport systems. A number of channels, pumps and symporters are affected by agents that modify the actin network. As an example, cytochalasins have been found to stimulate Na^+-K^+-$2Cl^-$ cotransport [75] and to activate the Na^+/K^+-ATPase [76], while some K^+ channels are inactivated by this treatment [77]. Phalloidin can inhibit K^+ and Na^+ channels [78,79] and jasplakinolide prevented the activation of Cl^- secretion induced by cAMP [75].

In addition to actin, the microtubule network is also a well-known constituent of the cortical cytoskeleton. Soluble tubulin has been found associated to the plasma membrane, and it is believed that this interaction may be the result of its binding to integral plasma membrane proteins [80]. Although it has been shown that acetylated tubulin can bind and inhibit PMCA activity [18], the effect of changes in microtubule dynamics, specially its depolymerization had not been addressed yet. Taking advantage of our experimental system to measure the effect of microtubule depolymerization induced by colchicine on PMCA activity, we found that microtubule depolymerization led to PMCA activation, very likely by rising the tubulin pool in the cell which in turn forms a complex with the pump and inhibits it. However, we cannot rule out other possibilities that may account for the observed effect. It has been shown that the intracellular ATP level at the cell edge is influenced not only by actin dynamics but also – albeit to a lesser extent – by microtubule dynamics [73]. It was shown that treating cells with taxol – a microtubule stabilizer – increased ATP levels. Since we observed that colchicine inhibited PMCA activity, the effect of disrupting the microtubule network could also be explained by the effect of microtubules on ATP levels.

Lastly, a further level of complexity arises in this system if we consider crosstalk between the actin and microtubule cytoskeletons, which has been reported to occur during cell division, shape changes and migration [81,82]. The architecture of the cortical F-actin cytoskeleton can be regulated by microtubules via modulation of different effectors such as Rho GTPses. Conversely, feedback can also occur from the cortical actin cytoskeleton to alter microtubule stability. Thus, the state of PMCA activation/inhibition may be the result of this complex actin/microtubule interaction dynamics.

5. Conclusion

In the present work we provide evidence for the role of the cortical cytoskeleton – both, the actin and microtubule systems – in modulating the PMCA activity in a living cell system. Moreover, this is the first time that PMCA2 is shown to be regulated by actin. Together with our previous reports, this suggests that regulation by the actin cytoskeleton may be a property shared by all PMCA isoforms.

Funding sources

This work was supported by Agencia Nacional de Promoción Científica y Tecnológica PICT 2012-2014 0065, Consejo Nacional de Investigaciones Científicas y Técnicas PIP 11220150100250CO, and Universidad de Buenos Aires Ciencia y Técnica grant 2014-2017: 20020130100254B (Argentina).

Author contributions

MGD, MFG, NM and AS conducted experiments. MGD, MAH and JPR designed the experiments. MGD and MFG performed data analysis and statistical evaluations. MGD, EES and JPR wrote the manuscript.

Conflict of interests

All authors declare that they have no conflict of interest.

Transparency document

The http://dx.doi.org/10.1016/j.bbamcr.2017.05.014 associated with this article can be found, in online version.

References

[1] E. Carafoli, Intracellular calcium homeostasis, Annu. Rev. Biochem. 56 (1987) 395–433.
[2] F.C. Mooren, R.K.H. Kinne, Cellular calcium in health and disease, Biochim. Biophys. Acta 1406 (1998) 127–151.
[3] M.J. Berridge, P. Lipp, M.D. Bootman, The versatility and universality of calcium signaling, Nat. Rev. Mol. Cell Biol. 1 (2000) 11–21.
[4] M.J. Berridge, M.D. Bootman, H.L. Roderick, Calcium signaling: dynamics, homeostasis and remodeling, Nat. Rev. Mol. Cell Biol. 4 (2003) 517–529.
[5] B. Sarkadi, Active calcium transport in human red cells, Biochim. Biophys. Acta 604 (1980) 159–190.
[6] H.J. Schatzmann, The plasma membrane calcium pump of erythrocytes and other animal cells, in: E. Carafoli (Ed.), Membrane Transport of Calcium, Academic Press, London, 1982, pp. 41–108.
[7] F. Di Leva, T. Domi, L. Fedrizzi, D. Lim, E. Carafoli, The plasma membrane Ca^{2+} ATPase of animal cells: structure, function, and regulation, Arch. Biochem. Biophys. 476 (2008) 65–74.
[8] E. Carafoli, Calcium pump of the plasma membrane, Physiol. Rev. 71 (1991) 129–153.
[9] M. Brini, L. Coletto, N. Pierobon, N. Kraev, D. Guerini, et al., A comparative functional analysis of plasma membrane Ca^{2+} pump isoforms in intact cells, J. Biol. Chem. 278 (2003) 24500–24508.
[10] E.E. Strehler, Plasma membrane calcium ATPases: from generic Ca^{2+} sump pumps to versatile systems for fine-tuning cellular Ca^{2+}, Biochem. Biophys. Res. Commun. 460 (2015) 26–33.
[11] R. Falchetto, T. Vorherr, J. Brunner, E. Carafoli, The plasma membrane Ca^{2+} pump contains a site that interacts with its calmodulin-binding domain, J. Biol. Chem. 266 (1991) 2930–2936.
[12] R. Falchetto, T. Vorherr, E. Carafoli, The calmodulin-binding site of the plasma membrane Ca^{2+} pump interacts with the transduction domain of the enzyme, Protein Sci. 1 (1992) 1613–1621.
[13] A. Enyedi, M. Flura, B. Sarkadi, G. Gardos, E. Carafoli, The maximal velocity and the calcium affinity of the red cell calcium pump may be regulated independently, J. Biol. Chem. 262 (1987) 6425–6430.
[14] V. Niggli, E.S. Adunyah, E. Carafoli, Acidic PL, unsaturated fatty acids, and limited proteolysis mimic the effect of calmodulin on the purified erythrocyte Ca^{2+}-ATPase, J. Biol. Chem. 256 (1981) 8588–8592.
[15] L. Vanagas, M.C. de La Fuente, M. Dalghi, M. Ferreira-Gomes, R.C. Rossi, et al., Differential effects of G- and F-actin on the plasma membrane calcium pump activity, Cell Biochem. Biophys. 66 (2013) 187–198.
[16] M.G. Dalghi, M.M. Fernández, M. Ferreira-Gomes, I.C. Mangialavori, E.L. Malchiodi, et al., Plasma membrane calcium ATPase activity is regulated by actin oligomers through direct interaction, J. Biol. Chem. 288 (2013) 23380–23393.
[17] S. Khurana, Role of actin cytoskeleton in regulation of ion transport: examples from epithelial cells, J. Membr. Biol. 178 (2000) 73–87.
[18] N.E. Monesterolo, V.S. Santander, A.N. Campetelli, C.A. Arce, H.S. Barra, et al., Activation of PMCA by calmodulin or ethanol in plasma membrane vesicles from rat brain involves dissociation of the acetylated tubulin/PMCA complex, FEBS J. 275 (2008) 3567–3579.
[19] M.C. Chicka, E.E. Strehler, Alternative splicing of the first intracellular loop of

plasma membrane Ca^{2+}-ATPase isoform 2 alters its membrane targeting, J. Biol. Chem. 278 (2003) 18464–18470.
[20] H.P. Adamo, A.K. Verma, R. Sanders, R. Heim, J.J. Salisbury, et al., Overexpression of the erythrocyte plasma membrane Ca^{2+} pump in COS-1 cells, Biochem. J. 285 (1992) 791–797.
[21] N. Montalbetti, A. Simonin, M.G. Dalghi, G. Kovacs, M.A. Hediger, Development and validation of a fast and homogenous cell-based fluorescence screening assay for divalent metal transporter 1 (DMT1/SLC11A2) using the FLIPR Tetra, J. Biomol. Screen. 19 (2014) 900–908.
[22] C.V. Filomatori, A.F. Rega, On the mechanism of activation of the plasma membrane Ca^{2+}-ATPase by ATP and acidic phospholipids, J. Biol. Chem. 278 (2003) 22265–22271.
[23] C.H. Fiske, Y. Subbarow, The colorimetric determination of phosphorous, J. Biol. Chem. 1479 (1925) 66–71.
[24] W.C. Chang, C. Nelson, A.B. Parekh, Ca^{2+} influx through CRAC channels activates cytosolic phospholipase A2, leukotriene C4 secretion, and expression of c-fos through ERK-dependent and -independent pathways in mast cells, FASEB J. 20 (2006) 2381–2383.
[25] D.M.F. Cooper, M. Yoshimura, X.Y. Zhang, M. Chiono, R. Mahey, Capacitative Ca2 + entry regulates Ca^{2+}-sensitive adenylyl cyclases, Biochem. J. 297 (1994) 437–440.
[26] S.W. Ng, C. Nelson, A.B. Parekh, Coupling of Ca^{2+} microdomains to spatially and temporally distinct cellular responses by the tyrosine kinase Syk, J. Biol. Chem. 284 (2009) 24767–24772.
[27] J.W. Putney, The physiological function of store-operated calcium entry, Neurochem. Res. 36 (2011) 1157–1165.
[28] O. Thastrup, P.J. Cullen, B.K. Drobak, M.R. Hanley, A.P. Dawson, Thapsigargin, a tumor promoter, discharges intracellular Ca^{2+} stores by specific inhibition of the endoplasmic reticulum Ca^{2+}-ATPase, Proc. Natl. Acad. Sci. U. S. A. 87 (1990) 2466–2470.
[29] J. Lytton, M. Westlin, M.R. Hanley, Thapsigargin inhibits the sarcoplasmic or endoplasmic reticulum Ca-ATPase family of calcium pumps, J. Biol. Chem. 266 (1991) 17067–17071.
[30] H. Takemura, A.R. Hughes, O. Thastrup, J.W. Putney, Activation of calcium entry by the tumor promoter, thapsigargin, in parotid acinar cells. Evidence that an intracellular calcium pool, and not an inositol phosphate, regulates calcium fluxes at the plasma membrane, J. Biol. Chem. 264 (1989) 12266–12271.
[31] A.B. Parekh, J.W. Putney Jr., Store-operated calcium channels, Physiol. Rev. 85 (2005) 757–810.
[32] A. Riccio, C. Mattei, R.E. Kelsell, A.D. Medhurst, A.R. Calver, et al., Cloning and functional expression of human short TRP7, a candidate protein for store-operated Ca^{2+} influx, J. Biol. Chem. 277 (2002) 12302–12309.
[33] Y. Liao, C. Erxleben, E. Yildirim, J. Abramowitz, D.L. Armstrong, et al., Orai proteins interact with TRPC channels and confer responsiveness to store depletion, Proc. Natl. Acad. Sci. 104 (2007) 4682–4687.
[34] Q.K. Tran, M. VerMeer, M.A. Burgard, A.B. Hassan, J. Giles, Hetero-oligomeric complex between the G protein-coupled estrogen receptor 1 and the plasma membrane Ca^{2+}-ATPase 4b, J. Biol. Chem. 290 (2015) 13293–13307.
[35] H. Hilfiker, D. Guerini, E. Carafoli, Cloning and expression of isoform 2 of the human plasma membrane Ca^{2+} ATPase. Functional properties of the enzyme and its splicing products, J. Biol. Chem. 269 (1994) 26178–26183.
[36] E.E. Strehler, D.A. Zacharias, Role of alternative splicing in generating isoform diversity among plasma membrane calcium pumps, Physiol. Rev. 81 (2001) 21–50.
[37] K. Pászty, A.J. Caride, Z. Bajzer, C.P. Offord, R. Padányi, et al., Plasma membrane Ca^{2+}-ATPase can shape the pattern of Ca^{2+} transients induced by store-operated Ca^{2+} entry, Sci. Signal. 8 (2015) ra19.
[38] G. Antalffy, K. Pászty, K. Varga, L. Hegedus, A. Enyedi, et al., A C-terminal di-leucine motif controls plasma membrane expression of PMCA4b, Biochim. Biophys. Acta 1833 (2013) 2561–2572.
[39] M.F. Ritchie, E. Samakai, J. Soboloff, STIM1 is required for attenuation of PMCA-mediated Ca^{2+} clearance during T-cell activation, EMBO J. 31 (2012) 1123–1133.
[40] S.S. Brown, J.A. Spudich, Cytochalasin inhibits the rate of elongation of actin filament fragments, J. Cell Biol. 83 (1979) 657–662.
[41] S.S. Brown, J.A. Spudich, Mechanism of action of cytochalasin: evidence that it binds to actin filament ends, J. Cell Biol. 88 (1981) 487–491.
[42] C. Galán, N. Dionisio, T. Smani, G.M. Salido, J.A. Rosado, The cytoskeleton plays a modulatory role in the association between STIM1 and the Ca^{2+} cannel subunit Orai1 and TRPC1, Biochem. Pharmacol. 82 (2011) 400–410.
[43] P. Mueller, D. Quintana, D. Griesemer, M. Hoth, J. Pieters, Disruption of the cortical actin cytoskeleton does not affect store operated Ca^{2+} channels in human T-cells, FEBS Lett. 581 (2007) 3557–3562.
[44] R.L. Patterson, D.B. van Rossum, D.L. Gill, Store-operated Ca^{2+} entry: evidence for a secretion-like coupling model, Cell 98 (1999) 487–499.
[45] D. Bakowski, M.D. Glitsch, A.B. Parekh, An examination of the secretion-like coupling model for the activation of the Ca^{2+} released-activated Ca^{2+} current I (CRAC) in RBL-1 cells, J. Physiol. 532 (2001) 55–71.
[46] J.R. Holda, L.A. Blatter, Capacitative calcium entry is inhibited in vascular endothelial cells by disruption of cytoskeletal microfilaments, FEBS Lett. 403 (1997) 191–196.
[47] P. Wales, C.E. Schuberth, R. Aufschnaiter, J. Fels, I. García-Aguilar, et al., Calcium-mediated actin reset (CaAR) mediates acute cell adaptations, elife 5 (2016), http://dx.doi.org/10.7554/eLife.19850.
[48] F.V. Rivas, J.P. O'Keefe, M.L. Alegre, T.F. Gajewski, Actin cytoskeleton regulates calcium dynamics and NFAT nuclear duration, Mol. Cell. Biol. 24 (2004) 1628–1639.
[49] M.R. Bubb, A.M.J. Senderowicz, E.A. Sausville, K.L.K. Duncan, E.D. Korn, Jasplakinolide, a cytotoxic product, induces actin polymerization and competitively inhibits the binding of phalloidin to F-actin, J. Biol. Chem. 269 (1994) 14869–14871.
[50] M.R. Bubb, I. Spector, B.B. Beyer, K.M. Fosen, Effects of jasplakinolide on the kinetics of actin polymerization. An explanation for certain in vivo observations, J. Biol. Chem. 275 (2000) 5163–5170.
[51] Y. Tu, S. Wu, X. Shi, K. Chen, C. Wu, Migfilin and Mig-2 link focal adhesions to filamin and the actin cytoskeleton and function in cell shape modulation, Cell 113 (2003) 37–47.
[52] S.B. Hastie, Interactions of colchicine with tubulin, Pharmacol. Ther. 51 (1991) 377–401.
[53] D.A. Skoufias, L. Wilson, Mechanism of inhibition of microtubule polymerization by colchicine: inhibitory potencies of unliganded colchicine and tubulin-colchicine complexes, Biochemistry 3 (1992) 738–746.
[54] R.B. Ravelli, B. Gigant, P.A. Curmi, I. Jourdain, S. Lachkar, et al., Insight into tubulin regulation from a complex with colchicine and a stathmin-like domain, Nature 428 (2004) 198–202.
[55] C.M. Ribeiro, J. Reece, J.W. Putney Jr., Role of the cytoskeleton in calcium signaling in NIH 3T3 cells. An intact cytoskeleton is required for agonist-induced [Ca^{2+}]i signaling, but not for capacitative calcium entry, J. Biol. Chem. 272 (1997) 26555–26561.
[56] J.T. Smyth, W.I. DeHaven, G.S. Bird, J.W. Putney Jr., Role of the microtubule cytoskeleton in the function of the store-operated Ca^{2+} channel activator STIM1, J. Cell Sci. 120 (2007) 3762–3771.
[57] L.G. Cao, D.J. Fishkind, Y.L. Wang, Localization and dynamics of nonfilamentous actin in cultured cells, J. Cell Biol. 123 (1993) 173–181.
[58] A. Spudich, J.T. Wrenn, N.K. Wessells, Unfertilized sea urchin eggs contain a discrete cortical shell of actin that is subdivided into two organizational states, Cell Motil. Cytoskeleton 9 (1988) 85–96.
[59] X. Shao, Q. Li, A. Mogilner, A.D. Bershadsky, G.V. Shivashankar, Mechanical stimulation induces formin-dependent assembly of a perinuclear actin rim, Proc. Natl. Acad. Sci. U. S. A. 112 (2015) E2595–E2601.
[60] H.L. Yin, J.H. Hartwig, K. Maruyama, T.P. Stossel, Ca^{2+} control of actin filament length. Effects of macrophage gelsolin on actin polymerization, J. Biol. Chem. 256 (1981) 9693–9697.
[61] A. Bretscher, K. Weber, Villin is a major protein of the microvillus cytoskeleton which binds both G and F actin in a calcium-dependent manner, Cell 200 (1980) 839–847.
[62] H.Y. Kueh, G.T. Charra, T.J. Mitchison, W.M. Brieher, Actin disassembly by cofilin, coronin, and Aip1 occurs in bursts and is inhibited by barbed-end cappers, J. Cell Biol. 182 (2008) 341–353.
[63] N. Joseph, B. Reicher, M. Barda-Saad, The calcium feedback loop and T cell activation: how cytoskeleton networks control intracellular calcium flux, Biochim. Biophys. Acta 1838 (2014) 557–568.
[64] R. Padányi, K. Pászty, E.E. Strehler, A. Enyedi, PSD-95 mediates membrane clustering of the human plasma membrane Ca^{2+} pump isoform 4b, Biochim. Biophys. Acta 1793 (2009) 1023–1032.
[65] D. Kosk-Kosicka, T. Bzdega, Activation of the erythrocyte Ca^{2+}-ATPase by either self-association or interaction with calmodulin, J. Biol. Chem. 263 (1988) 18184–18189.
[66] D. Kosk-Kosicka, T. Bzdega, A. Wawrynow, Fluorescence energy transfer studies of purified erythrocyte Ca^{2+}-ATPase. Ca^{2+}-regulated activation by oligomerization, J. Biol. Chem. 264 (1989) 19495–19499.
[67] D.L. Sackett, D. Kosk-Kosicka, The active species of plasma membrane Ca^{2+}-ATPase are a dimer and a monomer-calmodulin complex, J. Biol. Chem. 271 (1996) 9987–9991.
[68] L.J. Pike, L. Casey, Localization and turnover of phosphatidylinositol 4,5-bisphosphate in caveolin-enriched membrane domains, J. Biol. Chem. 271 (1996) 26453–26456.
[69] P.W. Shaul, E.J. Smart, L.J. Robinson, Z. German, I.S. Yuhanna, et al., Acylation targets endothelial nitric-oxide synthase to plasmalemmal caveolae, J. Biol. Chem. 271 (1996) 6518–6522.
[70] V. Niggli, E.S. Adunyah, J.T. Penniston, E. Carafoli, Purified (Ca^{2+}-Mg^{2+})-ATPase of the erythrocyte membrane. Reconstitution and effect of calmodulin and phospholipids, J. Biol. Chem. 256 (1981) 395–401.
[71] H.L. Yin, P.A. Janmey, Phosphoinositide regulation of the actin cytoskeleton, Annu. Rev. Physiol. 65 (2003) 761–789.
[72] L. Vanagas, R.C. Rossi, A.J. Caride, A.G. Filoteo, E.E. Strehler, et al., Plasma membrane calcium pump activity is affected by the membrane protein concentration: evidence for the involvement of the actin cytoskeleton, Biochim. Biophys. Acta 1768 (2007) 1641–1649.
[73] R. Suzuki, K. Hotta, K. Oka, Spatiotemporal quantification of subcellular ATP levels in a single HeLa cell during changes in morphology, Sci. Rep. 5 (2015) 16874.
[74] H. Imamura, K.P. Nhat, H. Togawa, K. Saito, R. Iino, et al., Visualization of ATP levels inside single living cells with fluorescence resonance energy transfer-based genetically encoded indicators, Proc. Natl. Acad. Sci. U. S. A. 106 (2009) 15651–15656.
[75] J.B. Matthews, J.A. Smith, B.J. Hrnjez, Effects of F-actin stabilization or disassembly on epitelial Cl-secretion and Na-K-2Cl cotransport, Am. J. Phys. 272 (1997) C254–C262.
[76] H.F. Cantiello, Actin filaments stimulate the Na(+)-K(+)-ATPase, Am. J. Phys. 269 (1995) F637–F643.
[77] U.R. Mauerer, E.L. Boulpaep, A.S. Segal, Regulation of an inward rectifying ATP-sensitive K^+ channel in the basolateral membrane of renal proximal tubule, J. Gen. Physiol. 111 (1998) 161–180.
[78] W.H. Wang, A. Cassola, G. Giebisch, Involvement of actin cytoskeleton in

modulation of apical K channel activity in rat collecting duct, Am. J. Phys. 267 (1994) F592–F598.
[79] B.K. Berdiev, A.G. Prat, H.F. Cantiello, D.A. Ausiello, C.M. Fuller, et al., Regulation of epithelial sodium channels by short actin filaments, J. Biol. Chem. 271 (1996) 17704–17710.
[80] A.C. Alonso, M. Nuñez-Fernandez, D.M. Beltramo, C.H. Casale, H.S. Barra, Na +, K +-ATPase was found to be the membrane component responsible for the hydrophobic behavior of the brain membrane tubulin, Biochem. Biophys. Res. Commun. 253 (1998) 824–827.
[81] T.K. Akhshi, D. Wernike, A. Piekny, Microtubules and actin crosstalk in cell migration and division, Cytoskeleton (Hoboken) 71 (2014) 1–23.
[82] G.M. Cammarata, E.A. Bearce, L.A. Lowery, Cytoskeletal social networking in the growth cone: how + TIPs mediate microtubule-actin cross-linking to drive axon outgrowth and guiadance, Cytoskeleton (Hoboken) 73 (2016) 461–476.